Thermal and kinetic constraints on the tectonic applications of thermobarometry

PETER D. CROWLEY

Department of Geology, Amherst College, Amherst, MA 01002, U.S.A.

AND

Geologisches Institut, ETH-Zentrum, CH-8092 Zürich, Switzerland

Abstract

Metamorphic petrology, and in particular quantitative thermobarometry, offer the possibility of identifying faults in metamorphic terrains by the metamorphic and/or thermobarometric breaks that occur across them. Furthermore, the sense of the thermobarometric break (e.g. warmer, deeper rocks on top of colder, shallower ones) and its magnitude could be useful tools for determining the sense and magnitude of the fault. The sensitivity of thermobarometry to tectonic variables such as fault throw and uplift rate, has been tested by a series of one-dimensional numerical re-equilibration models for both thrust and normal faults. In each of these models, the post-tectonic re-equilibration of a model garnet–biotite geothermometer is simulated by coupling one-dimensional numerical thermal and garnet diffusion models. After cooling and uplift, a thermobarometric temperature was calculated by using a near-rim garnet composition (5–10 μm from the rim) calculated by the re-equilibration model and biotite from the model matrix. The models varied the thermal structure of the model orogen prior to faulting, the depth of the fault, the structural throw of the fault, and the uplift rate following faulting.

All models produced zoned garnet porphyroblasts that recorded *P–T* conditions that were different from those at the time of fault motion. Most of the models produced thermobarometric breaks that were in the same sense as the temperature break at the time of fault motion. Normal faults produced a normal thermobarometric gradient with higher temperatures recorded below the fault than above it. Many, but not all of the thrust models produced a thermobarometric inversion near the fault, with higher temperatures locally recorded above the fault than below it. However, the magnitude of thermobarometric break correlated poorly with the fault throw. Most models developed thermobarometric breaks that were much smaller than the breaks that existed at the time of fault motion. The size of the thermobarometric break was commonly of the same magnitude as would be generated from microprobe analytical error. The models suggest that for metamorphic rocks whose thermal peak does not exceed a narrowly defined closure temperature, thermobarometry faithfully recorded the *P–T* conditions of the metamorphic peak. The closure temperature increases slightly with increasing uplift rate, but overall is rather insensitive to the uplift rate or other tectonic variables. For rocks whose thermal peaks is above the closure temperature, however, the model thermobarometer recorded a temperature that was very close to the closure temperature.

KEYWORDS: thermobarometry, faults, metamorphic petrology, garnet–biotite geothermometer.

Introduction

METAMORPHIC ROCKS are generally exposed in structurally complex terranes in which low-angle faults and tight folds are common. Even in the best studied metamorphic terranes, the stratigraphy is not well known, as synmetamorphic deformation commonly obliterates both fossils and primary structures indicative of the facing direction. In many metamorphic terranes, the discovery of previously unrecognized low-angle thrust and normal faults have produced stratigraphic revisions. It is often difficult to recognize these low-angle faults, however, because of the ambiguities in stratigraphy. For this reason, abrupt variations in metamorphic mineral assemblages and/or the pressure and temperature calculated by geothermobarometry have been

Mineralogical Magazine, March 1991, Vol. 55, pp. 57–69

useful to delineate the location of low-angle faults (Mancktelow, 1985; Crowley and Spear, 1987; Rice *et al.*, 1989).

Petrologists continue to improve the calibrations of thermobarometric equilibria (e.g. Koziol and Newton, 1988) and to debate about the details of mineral solution models. Even so, there exists a wide variety of reliable geothermobarometers for metamorphic rocks that are based on continuous net-transfer or exchange equilibria (Essene, 1989, and references therein). Geothermobarometry therefore offers the possibility of being a useful tool to geologists for sorting out structural or stratigraphic problems in metamorphic terranes. In particular, thermobarometry offers the possibility of quantitatively estimating the pressure and temperature of equilibration. Breaks, or abnormally steep gradients in thermobarometric P–T, may help delimit the location of low-angle faults, indicate their nature (reverse or normal), and provide a means of quantitatively estimating the amount of structural throw across such faults.

Unfortunately, tectonic applications of thermobarometry are far from simple, because the very structural events in which we are interested will cause rocks in a metamorphic terrane to follow complex P–T paths (England and Richardson, 1977; England and Thompson, 1984; Buck *et al.*, 1988). At some point along this complex P–T path, the pressure and/or temperature recorded by a thermobarometer will be frozen into the rocks. This point is likely to occur at different times in rocks that have followed different P–T paths.

The reaction mechanisms by which the mineral assemblages used for thermobarometry re-equilibrate while tracking such a P–T path are poorly known. Under different conditions, dissolution of a reactant phase, material transport within an individual phase (volume diffusion), material transport between phases (intergranular diffusion) or the precipitation of a produce phase may be rate limiting (Fisher, 1978; Walther and Wood, 1984). Even if the rate-limiting mechanism can be identified, quantitative rate laws describing the kinetics of re-equilibration are not well known.

It is clear, however, that intracrystalline or volume diffusion is an important and potentially rate-limiting step in the re-equilibration process, particularly for exchange reactions. Furthermore, the mathematics of volume diffusion is well understood and suitable to both analytical and numerical solution (Crank, 1975) and a wide range of diffusion constants for many common minerals (Freer, 1981) have been determined. For these reasons, previous studies (Dodson, 1973; Lasaga *et al.*, 1977; Lasaga, 1983) have used volume diffusion to quantitatively model the kinetics of mineral re-equilibration.

Dodson (1973) demonstrated that, due to the exponential dependence of diffusion rates on temperature, there is a narrow temperature interval over which equilibration of an exchange reaction will cease during cooling from a thermal maximum. Above a critical temperature, the closure temperature, re-equilibration will be fast enough to be able to keep up with P–T changes, whereas at temperatures below the closure temperature, re-equilibration effectively ceases. In Dodson's formulation, the closure temperature of a phase to volume diffusion increases as the cooling rate increases. Lasaga *et al.* (1977) and Lasage (1983) further considered the importance of interdiffusion on the re-equilibration of exchange equilibria and developed the concept of geospeedometry, in which the importance of the cooling rate on the temperature and pressure recorded by thermobarometers was emphasized. Both Dodson (1973) and Lasaga (1983) attempted to place geologically reasonable boundary conditions on the diffusion equation and then generated analytical solutions to the equations. In order to analytically solve the diffusion equation, both Dodson and Lasaga had to assume relatively simple thermal histories. Both assume that orogenic terranes followed nearly linear cooling paths after a thermal peak. Numerical thermal models for the evolution of metamorphic terranes (Thompson and England, 1984) suggest that even simple tectonic histories can cause rocks to follow P–T paths along which the cooling rate for a single rock can vary by orders of magnitude following the metamorphic peak. Inasmuch as cooling rate is the only tectonic variable in Dodson's and Lasaga's analytical solutions, numerical thermal models suggest that a simple linear cooling path may be an oversimplification.

This paper presents a series of numerical models that attempt to simulate the P–T evolution of a metamorphic terrane following movement along a hypothetical low-angle fault. The models investigate the effect of the complex P–T path followed by the terrane on the re-equilibration by volume diffusion of a model geothermobarometer based on the Ferry and Spear (1978) garnet–biotite Fe–Mg exchange geothermometer. The models predict the point along a P–T path that will be recorded by the model thermobarometer, thus allowing us to quantitatively evaluate the utility of geothermobarometry in extracting tectonic information from a meta-

Table 1: Thermal constants used in the reequilibration models

Thermal conductivity	2.25	W/m/°K
Thermal diffusivity	0.9	μ m²/sec
Heat productivity	2.0	μW/m³
Basal heat flux	30	mW/m²

Model #'s	Thickness heat prod layer (km)	Fault type	Fault throw (km)	Fault depth (km)	Uplift rates (mm/ yr)
1 to 6	25	thrust	15	25	0.1 to 5.0
7 to 12	25	thrust	10	25	0.1 to 5.0
13 to 18	25	thrust	5	25	0.1 to 5.0
19 to 24	20	normal	15	25	0.1 to 5.0
25 to 30	20	normal	10	25	0.1 to 5.0
31 to 36	20	normal	5	25	0.1 to 5.0
37 to 42	20	normal	10	20	0.1 to 5.0
43 to 48	15	normal	15	20	0.1 to 5.0

morphic terrane. Specifically, the modelling was designed to see if: (1) the pressure and temperature recorded by thermobarometry can be used to estimate the sense and magnitude of displacement of faults in metamorphic terranes, and (2) how much the pressure and temperature recorded by thermobarometry is affected by variations in uplift rate. The quantitative results of the numerical models are strictly applicable only to the garnet–biotite exchange equilibria. However, similar boundary conditions and rate constants should govern the re-equilibration of other thermobarometers. The models discussed here therefore have implications that are qualitatively applicable to all exchange thermobarometers.

Description of the models

The thermal evolution of a hypothetical metamorphic terrane was simulated by a series of one-dimensional numerical thermal models. These models are explicit finite difference solutions to the one-dimensional heat flow equation with internal heat sources in an advecting reference frame (see England and Richardson, 1977, or England and Thompson, 1984, for a discussion of this type of thermal model). The thermal constants used in the models (Table 1) are similar to those of England and Thompson (1984) and were chosen to approximate the thermal structure of normal continental crust. The finite difference array was calculated to a depth of 100 km with distance steps spaced 1 km apart. Time steps were very short (20 Ka) to avoid stability problems with both the heat flow and diffusion equations. Increasing the depth of the array, decreasing the distance spacing of the grid points or decreasing the size of the time steps increases calculation time but has no significant impact on the results.

All of the models start with a steady-state geotherm that is in equilibrium with a basal heat flux from the mantle (at the base of the 100 km finite difference array) and with the production of heat in a radioactive heat-producing layer in the upper part of the continental crust. The thickness of the heat-producing layer varies among the models from 15 to 25 km in order to produce a thermal structure conducive to the creation of amphibolite-facies metamorphic *P–T* conditions in both the upper and lower plates of the model fault. Depending on the thickness of the heat-producing layer, the initial temperature at the base of a 30 km thick crust varied between 516 and 700 °C.

Each of the models began with the instantaneous movements on a crustal-scale fault. The structural throw on the faults varied from 5 to 15 km and both normal and reverse faults were simulated (Fig. 1). Fault motion instantaneously perturbed the initial equilibrium geotherm, producing a step in the geotherm. Following faulting, material was removed from the surface by erosion, uplifting the metamorphic terrane. Uplift occurred at a constant rate that ranged from 0.1 to 5 mm/yr. During uplift, the thermal evolution of rocks one finite difference grid point (1 km) above and below the fault were followed and depth–temperature paths for these rocks were constructed. Varying the thickness of the heat producing crustal layer, the uplift rate following faulting, and the depth and throw on the model fault produced *P–T* paths with thermal maxima that ranged from 465 to 740 °C. However, most of the models had amphibolite facies thermal peaks of approximately 540 to 675 °C. After each finite-

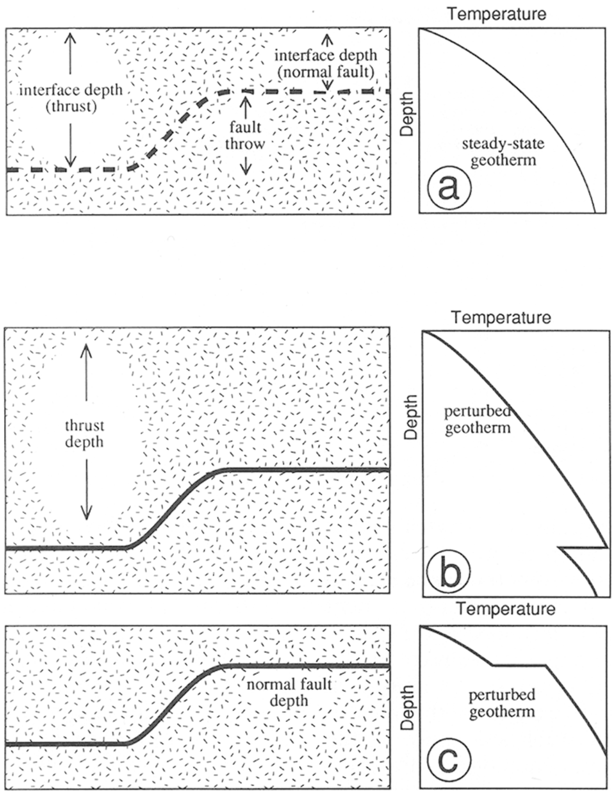

FIG. 1. Tectonic geometry and initial thermal structure considered in the thermal models. Instantaneous fault motion perturbs an initial steady-state geotherm producing a step-function geotherm. (*a*) Prior to faulting. (*b*) After thrust faulting, a hanging wall flat has moved up to a higher foot wall flat. (*c*) After normal faulting, a hanging wall flat has moved down to a structurally lower foot wall flat. The models considered faults at depths of 20 and 25 km with structural throws of 5, 10, and 15 km.

difference time step, the temperatures calculated by the thermal models were used as the input for a numerical diffusion model that simulated the re-equilibration of a garnet-biotite Fe–Mg exchange geothermometer.

The diffusion model simulated binary Fe–Mg interdiffusion between garnet and biotite. Although experimentally determined Fe–Mg interdiffusion constants for biotite are not available, comparison of the Mg diffusion coefficients for garnet and biotite (Cygan and Lasaga, 1985; Freer, 1981) suggests that under metamorphic *P–T* conditions, diffusion is greater than 5 orders of magnitude faster in biotite than it is in garnet. This difference is in accord with the observation that metamorphic garnet is commonly Fe–Mg zoned whereas biotite is not. The models discussed below assume that Fe–Mg diffusion in biotite is sufficiently fast that volume diffusion in garnet is rate-limiting. Thus, the kinetics of re-equilibration of the model thermobarometer are controlled by the kinetics of volume diffusion in garnet. Several diffusion coefficients for garnet appear in the literature (Lasaga *et al.*, 1977; Freer, 1981; Cygan and Lasaga, 1985; Elphick *et al.*, 1985). Each of the re-equilibration models was run three times using three different diffusion coefficients that spanned the range of available data. The values of these coefficients are listed in Table 2.

The models assumed that as temperature increases prior to the thermal peak garnet continued to grow and was able to equilibrate with matrix biotite. By the time the thermal peak was reached, each model had produced a homogeneous 1 mm garnet grain with a fixed Fe/Mg ratio [Fe/(Fe + Mg) = 0.8]. This Fe/(Fe + Mg) ratio is arbitrary, but was chosen to approximate a metamorphic garnet composition. At the thermal peak, this garnet was considered to be in chemical equilibrium with an infinite reservoir of matrix biotite. The Fe/Mg ratio of the reservoir of matrix

Table 2: Garnet diffusion data used in the reequilibration models.

source	type of data	D_0 m^2/sec	E_a kJ/mol
Lasaga et al., 1977	Fe-Mg interdiffusion	2.75×10^{-6}	293
Freer, 1981	Fe-Mg interdiffusion	6.11×10^{-4}	344
Cygan & Lasaga, 1985	Mg self diffusion	9.8×10^{-9}	239

$$D=D_0 \exp(-E_a/RT)$$

D_0- diffusion pre-exponential
E_a- activation energy
T- temperature (°K)
R- gas constant

biotite was controlled by the Fe–Mg partitioning of the garnet–biotite thermometer of Ferry and Spear (1978). In each time step after the thermal peak, the Fe/Mg ratio of the garnet rim was changed to maintain this Fe–Mg equilibrium. The change in garnet rim composition produced a chemical gradient which drove volume diffusion within the garnet. The composition of points within the garnet were calculated by a numerical diffusion model. This model is an explicit finite difference solution to the one-dimensional diffusion equation (Crank, 1975) in which the diffusion coefficient change with time as a result of changes in temperature calculated from the thermal model. The model assume that, for each time step, the diffusion coefficient is the same throughout the garnet grain and thus is independent of composition, although experimental studies of garnet diffusion (Elphick *et al.*, 1985) suggest that there is a slight compositional dependence on the Fe–Mg interdiffusion coefficient.

The models were stopped when the rock under consideration had cooled to 350 °C. At this temperature, diffusion in garnet had effectively ceased. Continuing the models to a temperature below this had no effect on the results. Garnet-biotite temperatures were then calculated by comparing the composition of the garnet a finite, but small distance in from the rim (both 5 and 10 μm from the rim) with the composition of the infinite biotite reservoir (Fig. 2). The garnet and biotite compositions used to calculate temperature simulate compositions that could be measured from adjacent grains by electron-microprobe and need not represent compositions that were ever in chemical equilibrium.

Simplifications implicit in the models. Due to the simplifications needed to mathematically model geological situations, numerical models should be considered to be a type of mathematical 'cartoon'. It is important to consider whether the simplifications needed to formulate the models have a major effect on the results. The following simplifications are implicit in the models: (1) One-dimensional thermal models ignore the lateral transport of heat; (2) Instantaneous fault movement is assumed whereas movement at plate tectonic rates requires emplacement times on the order of 1 million years; (3) An infinite reservoir of biotite is assumed whereas rocks can have only a finite amount; (4) The models start with an unzoned garnet grain whereas growth-zoned garnet is very common in nature; and (5) The models assume no migration of grain boundaries during re-equilibration whereas retrograde garnet resorption is common in nature. However, for the following reasons, these simplifications probably have only a minor effect on the results.

Two-dimensional thermal models and thermal models that account for finite fault displacement rates (e.g. Buck *et al.*, 1988; Ruppel *et al.*, 1988) yield results that are significantly different from one-dimensional models during the early stages of the models, particularly during and immediately following fault motion. After longer times, the differences between the one-dimensional and the more complex models are relatively small. Inasmuch as the re-equilibration that occurs in the models discussed here typically takes times on the order of tens of millions of years, the discrepancies that result from these simplifications should be minor.

Assuming the existence of an infinite reservoir of biotite is not unreasonable because, in common rock compositions, biotite is frequently a more abundant phase than garnet and thus acts as a large reservoir. Furthermore, in most of the models only a small part of the garnet, a thin (<100 μm) shell near the rim, exchanges Fe and Mg with the matrix biotite. The infinite reservoir assumption is useful because it simplifies the calculations by allowing the composition of the matrix biotite to remain unchanged throughout the evolution of a model. Changing to a finite amount of matrix biotite would have added mass balance calculations to the models. This is not difficult, but it would have reduced the generality of the models, as the results would have applied

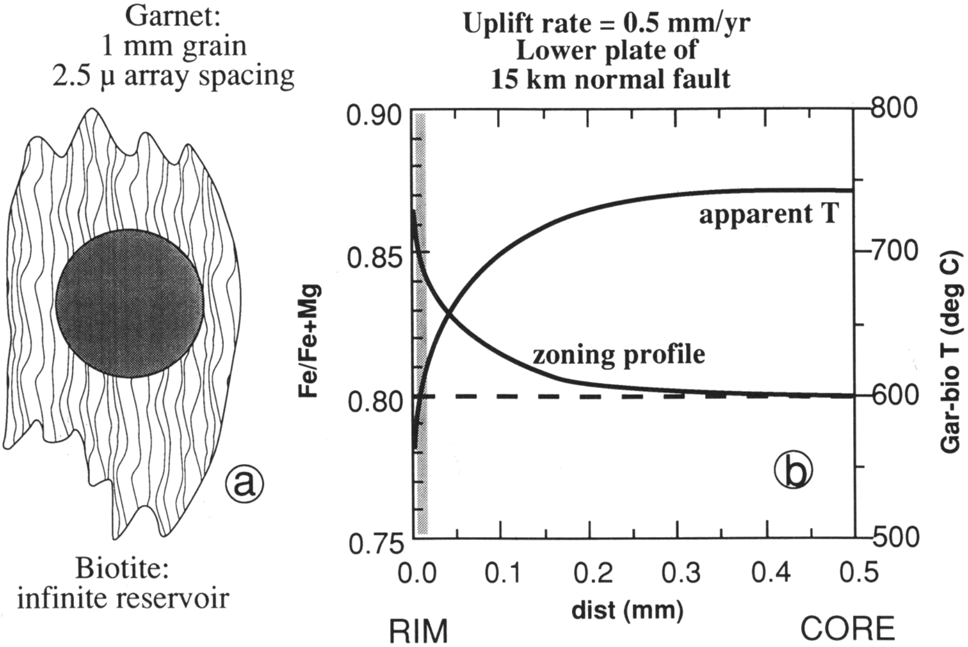

FIG. 2. (*a*) Geometry of diffusion-re-equilibration models. Garnet is considered to exchange Fe and Mg with an infinite reservoir of matrix biotite. The Fe/Mg ratio of the garnet rim is controlled by the partitioning described by the Ferry and Spear (1978) geothermometer. (*b*) Typical garnet zonation profile. The Fe/Mg ratio increases from core to rim. Temperatures are calculated by comparing the garnet composition with that of the reservoir of biotite. The dashed line represents the initial garnet composition.

only to specific relative abundances of garnet and biotite. Adding the mass balance calculations would have decreased the amount that the garnet rim composition changed in each model, as some of the compositional change needed to maintain the Fe–Mg partitioning is taken up by biotite. The zonation profiles calculated here therefore represent a maximum; rocks with a finite reservoir of matrix would be less strongly zoned.

The diffusion models did not start with zoned garnets because of uncertainties as to what to use as a starting zoning profile. Numerical experiments with initially zoned garnets, similar to natural garnets analysed by the author, produced diffusion profiles that were both steeper and shallower than the ones presented here. For similar reasons, garnet resorption during retrograde metamorphism was not considered. Although both of these may be important factors affecting the re-equilibration of a thermobarometer, it is not easy to include them in the models at present.

Results of the models

All of the models were run three times using different diffusion data (Table 2) to model garnet–biotite re-equilibration. Although the results of each of the three sets of simulations is quantitatively somewhat different, qualitatively they are very similar. Models calculated using the diffusion data of Freer (1981) which has the highest activation energy gave the highest garnet–biotite temperatures. For this reason, the models calculated with these data will be discussed below.

The thermal models produced depth-temperature (*P–T*) paths that are similar to those of other workers (England and Thompson, 1984; Davy and Gillet, 1986; Ruppel *et al.*, 1988; Connolly and Thompson, 1989). Fig. 3 shows a *P–T* path for a typical thrust fault model. Immediately following thrusting, rocks in the lower plate of the thrust heat up by the downward conduction of heat from the warmer upper plate. At the same time, the upper plate cools rapidly by conduction. As the perturbed geotherm relaxes during uplift, the lower plate slowly heats up with a steadily decreasing heating rate until the thermal maximum is reached. Following the thermal maximum, the lower plate cools along a path with a monotonically increasing cooling rate. The upper plate follows a more complicated path.

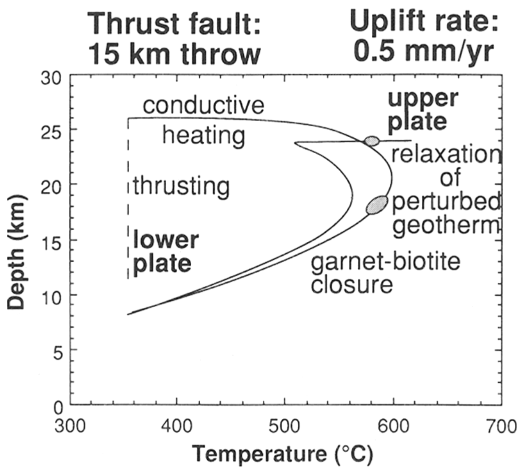

FIG. 3. Depth–temperature paths for a typical thrust-fault model. The lower plate is isothermally buried by thrusting (dashed line) and follows a clockwise path after thrusting. The model thermobarometer closes during uplift following the thermal peak. The upper plate first cools rapidly and then follows a clockwise path. The temperature recorded by the model thermobarometer reflect the conditions soon after thrusting. Shaded ellipses show the range in temperature recorded by the model thermobarometer. The slopes of the paths are inversely proportional to the heating/cooling rate.

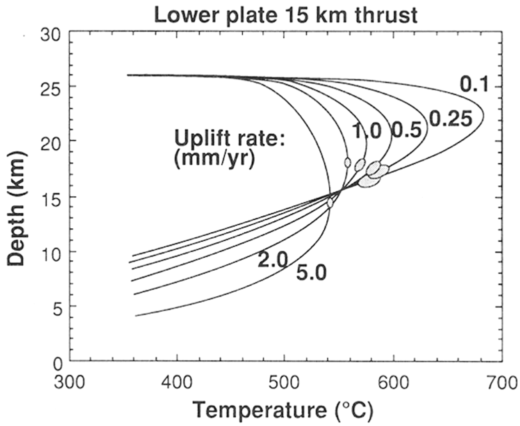

FIG. 4. Thrust model, lower plate. Shaded ellipses show the temperatures recorded by the model thermobarometer. With decreasing uplift rate, higher peak temperatures are reached. Regardless of the uplift rate, the thermobarometer records approximately similar temperatures.

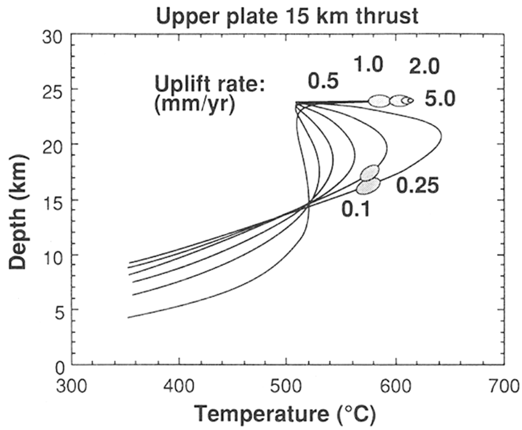

FIG. 5. Thrust model, upper plate. Shaded ellipses show the temperatures recorded by the model thermobarometer. With decreasing uplift rate, higher temperatures are reached during the clockwise part of the paths. Except at very slow uplift rates, the thermobarometer records conditions that were experienced very soon following thrusting.

Initially, the temperature decreases very rapidly as the upper plate conductively cools by heat transfer to the cooler lower plate. This cooling period is relatively short (<1 Ma) and then the upper plate begins to heat. For most models, the thermal peak of the upper plate occurred prior to thrusting. However, for models with low uplift rates, the thermal peak occurred after thrusting, during this heating phase. After this heating phase, the upper plate cooled along a path with a monotonically increasing cooling rate.

In all of the thrust models, lower plate rocks reach their thermal peak during post-faulting uplift, from 2.2 to 35 million years after fault motion. Cooling began slowly and diffusion was effective for some time following the thermal peak, so that the temperature recorded by thermobarometry was always lower than the peak temperature (Fig. 4). The discrepancy between the peak temperature and the temperature recorded by thermobarometry increases markedly as the uplift rate decreases. However, this effect is due more to the fact that higher peak temperatures were reached in rocks that came to the surface at lower uplift rates than to variations in the temperatures recorded by thermobarometry.

Except at very slow uplift rates (0.1 mm/yr), rocks in the upper plates of the thrust models were at their thermal peak at the time of thrusting. Although upper plate rocks remained hot enough for diffusion to be effective for up to ten's of Ma's following thrusting, the temperature calculated by thermobarometry generally reflects conditions experienced by the rocks very soon (<0.5 Ma) after thrusting (Fig. 5). As with the

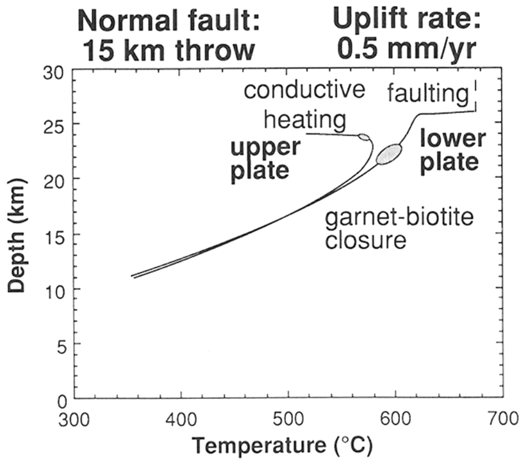

FIG. 6. Depth–temperature paths for a typical normal fault model. Shaded ellipses show the range in conditions recorded by the model thermobarometer. The lower plate is isothermally unroofed by instantaneous faulting (dashed line). The lower plate follows a cooling path after faulting. The thermobarometer closes during post-kinematic uplift. The upper plate follows a clockwise path after faulting with closure of the model thermobarometer occurring during uplift from the thermal peak.

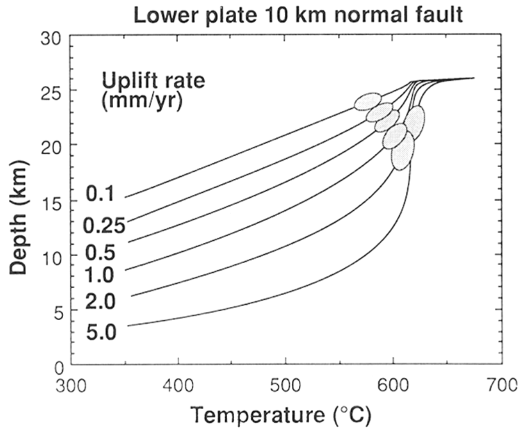

FIG. 7. Normal fault model, lower plate. Shaded ellipses show the temperatures recorded by the model thermobarometer. Increasing the uplift rate increases the cooling rate but otherwise the paths are similar. With increasing uplift rate, the temperature recorded by the thermobarometer also increases somewhat.

lower plate rocks, the upper plate rocks all record temperatures that are below the peak temperature. Again, the discrepancy between the peak temperature and the garnet–biotite temperature increases with decreasing uplift rate.

Fig. 6 shows the *P–T* path for a typical normal fault model. Immediately following fault motion, the rocks in the lower plate of the normal fault cool rapidly by the upward conductive of heat to the cool upper plate. At the same time, the upper plate heats rapidly. The upper plate reaches its thermal maximum soon (1.3 to 5 Ma) after fault motion. Following the thermal maximum, the upper plate cools with a steadily increasing cooling rate. The lower plate of the normal fault cools during the entire simulation. However, the cooling rate of the lower plate varies greatly during the simulation. Immediately following faulting it is very rapid (up to hundreds of °C/Ma), but soon decreases markedly to approximately 1 to 5 °C/Ma. Approximately 1.5 to 4 million years after fault motion, the cooling rate begins to increase again and then increases monotonically for the rest of the simulation.

In all of the normal fault models, the lower plate rocks were at their thermal peaks at the time of fault motion. Diffusion was effective for up to tens of millions of years following normal faulting. As a result of this, for all of the models the temperature recorded by thermobarometry is lower than the peak temperature. There is a small increase in the temperature recorded by thermobarometry at higher uplift rates (Fig. 7). Rocks in the upper plates of the normal fault simulations reached their thermal peaks soon after fault motion. In all cases, the temperature calculated by thermobarometry is lower than the peak temperature. However, variations in uplift rate had only a minor effect on either the peak or garnet–biotite temperatures of upper plate rocks (Fig. 8).

Discussion

At the time of fault motion, there was a large thermal difference across all of the simulated faults. The magnitude of the initial thermal difference increased with increases in the displacement across the model faults. For the thrust models, the temperature differences across faults with 5, 10, and 15 km of structural throw were 48, 145, and 265 °C respectively. The temperature differences across simulated normal faults with 5, 10 and 15 km of throw were 93, 160, and 226 °C respectively. If a thermobarometer closed prior to the time of fault motion preserving the Fe–Mg signature of this thermal break, it should be easily recognizable in the geological record as these differences are significantly larger than the ±25 °C that we would expect from analytical uncertainties (Hodges and Crowley, 1985; Hodges and McKenna, 1987). However, in none

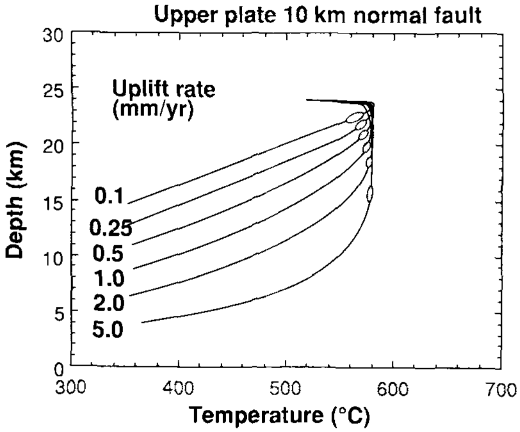

FIG. 8. Normal fault model, upper plate. Shaded ellipses show the temperatures recorded by the model thermobarometer. Regardless of the uplift rate, the peak temperatures and the temperature recorded by the thermobarometer are similar.

of the models was the initial thermal break across a fault faithfully recorded by thermobarometry. There are two reasons for this: the first is that the thermal peaks of rocks on opposite sides of the simulated faults are diachronous. Rocks from one side of the fault tend to be at their thermal peak at the time of fault motion, whereas rocks from the other fault block tend to reach their thermal peak after faulting. In all of the thrust models, rocks in the lower plate heated and reached their thermal peak following thrusting, whereas in all of the normal fault models, it was upper plate rocks that came to their thermal peak following faulting. The *P–T* conditions recorded by thermobarometry, therefore, do not reflect the *P–T* conditions at the time of faulting. The second reason that thermobarometry fails to faithfully record the thermal breaks is that temperatures in both plates were sufficiently high following motion for the model thermobarometer to partially re-equilibrate by volume diffusion.

In general, the thermobarometric breaks across the model faults were rather small. For almost all of the thrust models, and for many of the normal fault models, the thermobarometric break was less than 25 °C (Fig. 9). This is approximately the uncertainty generated by microprobe errors and could be difficult to recognize in nature.

The sense of movement indicated by the thermal break is generally correct. All of the normal fault models produce thermobarometric differences in which colder, shallower rocks sat on top of warmer, deeper rocks. On the other hand, not all of the thrust models produce the expected local inversion in thermobarometric temperature. Some of the thrust models produced normal *P–T* gradients in which cooler thermobarometric temperatures were recorded by upper plate rocks than by lower plate rocks. However, the thrust models that produced normal *P–T* gradients had very small thermobarometric differences across the faults. All of the thrust models with temperature differences greater than 10 °C produced thermobarometric breaks in which hotter upper plate rocks sat structurally above colder lower plate rocks.

The thermobarometric temperature difference across the faults varies greatly for faults with the same structural throw (Fig. 9). This suggests that the thermobarometric break is not a good quantitative indicator of the structural throw of a fault. Only for special structural geometries (Crowley, 1988) does thermobarometry seem capable of accurately recording the structural break.

Temperatures calculated with the model thermobarometer are very similar to the peak temperature as long as that thermal peak did not exceed a critical or closure temperature. The closure temperature for the models run using the Freer (1981) diffusion data (Fig. 10) is approximately 595 °C. For models that reach thermal peaks above this temperature, all of the model garnet–biotite temperatures are very close to the 595 °C closure temperature. There is a tendency for models run at a higher uplift rate to have a slightly higher closure temperature than those run at lower uplift rates However, this difference is relatively small (30–50 °C).

In general, these models suggest that the closure temperature concept of Dodson (1973), developed initially with a near linear cooling rates is applicable to geological terranes that follow complex *P–T* paths with cooling rates that vary by orders of magnitude. Due to these wide variations in cooling rate, direct comparisons between the closure temperatures calculated above and Dodson's closure temperature is not possible. However, the models suggest that the closure temperature is even less sensitive to changes uplift rate than to variations in cooling rate in Dodson's formulation, suggesting that closure temperature is almost independent of the tectonic scenario that produced a metamorphic terrane.

Sets of models run using the diffusion data of Lasaga *et al.* (1977) and Cygan and Lasaga (1985) gave similar results to those shown in Fig. 10, although the closure temperatures were different. The closure temperature calculated using the data of Lasaga *et al.* is slightly lower, approximately 570 °C, whereas that calculated from the data of Cygan and Lasaga is lower still, approximately 515 °C. In both of these sets of models, higher

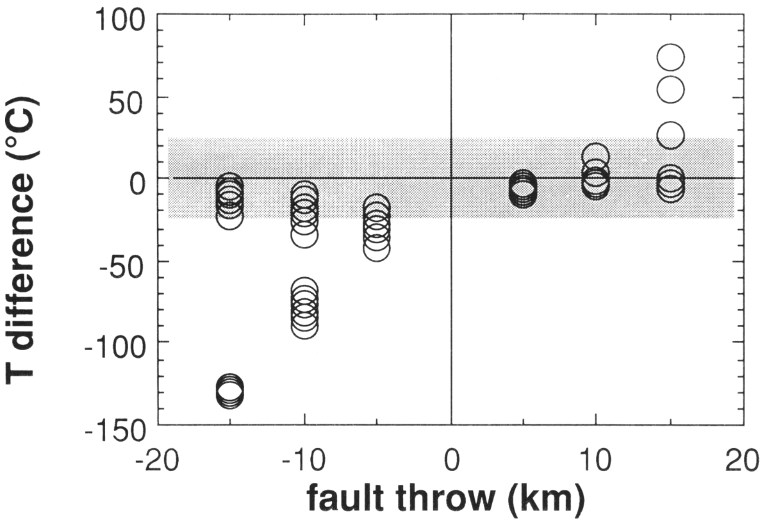

FIG. 9. Calculated thermobarometric difference (upper-plate–lower-plate) as a function of fault throw. A positive temperature difference corresponds to warmer rocks sitting on colder rocks whereas a positive fault throw corresponds to thrust motion. Most of the models produce differences in calculated temperature that are in the correct sense. However, most of them produce a thermobarometric break that falls within analytical uncertainty, the shaded ±25 temperature band.

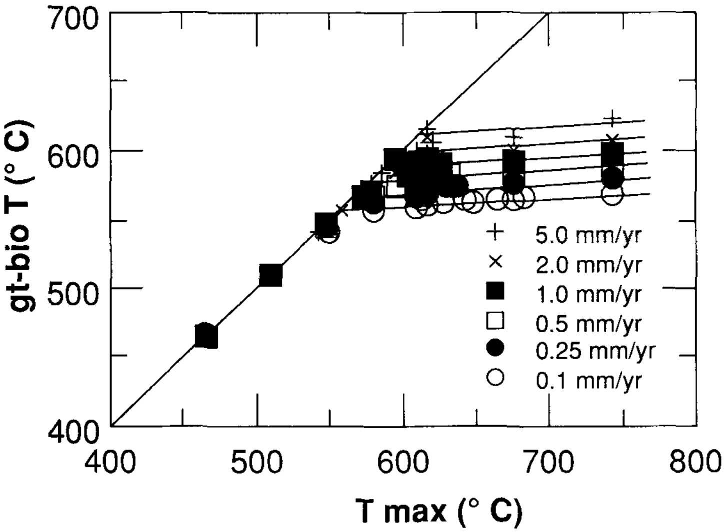

FIG. 10. Model garnet–biotite temperatures *vs.* maximum temperature. If the peak temperature exceeded the approximately 575–600 °C closure temperature of the model thermobarometer, a temperature close to the closure temperature was recorded. At higher uplift rates, slightly higher temperatures are recorded by the thermobarometer. Below the closure temperature, a temperature only slightly below T_{max} was recorded.

uplift rates produce higher closure temperatures. Due to the lower activation energies of both of these diffusion data, there is a somewhat larger spread in closure temperatures (50–75 °C) due to variations in the uplift rate.

This modelling indicates that the pressure or temperature recorded by a single exchange thermobarometer is controlled more by re-equilibration kinetics than by tectonic factors such as uplift rate. Frequently, thermobarometric pressure and temperature are calculated by the simultaneous solution of two or more continuous equilibria. The importance of kinetic factors rather than tectonic ones in determining the closure of a thermobarometer suggests that it is unlikely that two or more continuous reactions will close at the same time. The *P–T* calculated by simultaneous solution of several thermobarometers is likely to be meaningful only if the peak temperature did not exceed the closure temperatures for all of the equilibria.

The *P–T* conditions calculated in the models are relatively common in metamorphic belts in which magmatic heat has not perturbed the thermal structure. For example, in the northern Scandinavian Caledonides, garnet–biotite temperatures of approximately 570 to 600 °C are recorded by pelitic schists from a region that is thousands of square kilometers in size (Hodges and Royden, 1984; Crowley and Spear, 1987; Steltenpohl and Bartley, 1987; Barker and Anderson, 1989; Crowley, 1990). Although these rocks come from all levels of a nappe pile that presently is at least 10 km thick and were affected by multiple deformations during and after metamorphic mineral growth, they all record very similar temperatures. The thermal re-equilibration models presented here suggest that the similarity of *P–T* conditions recorded by thermobarometry over this wide region is due to the kinetics of re-equilibration during uplift, rather than similarities in tectonic or thermal history. These *P–T* conditions might be recorded regardless of the tectonic and thermal history.

Conclusions

The thermobarometry models presented here have many simplifications implicit in them that prevent direct quantitative application of the results to nature. However, they do serve as models to evaluate how much tectonic information can be gleaned from thermobarometry. In cases where a rock's thermal peak does not exceed the closure temperature for a particular thermobarometer, *P–T* conditions very close to the thermal peak should be recorded by thermobarometry. If the peak temperature is above the closure temperature, however, all rocks are likely to record conditions that are within analytical uncertainties of the closure temperature. In these cases, regardless of their tectonic histories, thermobarometry will record approximately the same conditions. Tectonic parameters such as the uplift rate or the proximity of faults that act as major heat sources or sinks may have only minor effects on the *P–T* recorded by thermobarometry.

Most of the models predicted the existence of a thermobarometric gradient across the faults that was in the correct sense. In other words, thrust fault models initially placed hot rocks on top of colder ones and thermobarometry recorded an inverted temperature gradient with higher temperatures locally found in upper plate rocks than in lower plate rocks. Normal fault models initially placed colder rocks on top of hotter ones and thermobarometry recorded a temperature gradient with higher temperatures in the lower plate than the upper plate. However, the magnitude of these breaks was rather small, generally in the range of uncertainty generated by microprobe errors. There was a very poor correlation between the magnitude of the thermobarometric breaks and the magnitude of the throw across the faults. Although thermobarometry may help delineate low-angle faults in metamorphic terranes, is not likely to be a good tool for evaluating the magnitude of displacement across them.

This study suggests that in many cases, the temperature or pressure recorded by thermobarometry will be influenced much more by kinetic factors than by tectonic ones. The three sets of models discussed here all considered re-equilibration to occur by the same diffusional mechanism, but each used slightly different diffusion data. Between the sets of models, closure temperature varied by approximately 75 °C, whereas, within any one set of models with differing tectonic histories, the closure temperature varied by a smaller amount, approximately 50 °C.

The mechanisms by which a metamorphic mineral assemblage equilibrates during prograde metamorphism or re-equilibrates during cooling are poorly known. Volume diffusion has been considered to be an important factor in the kinetics of retrograde re-equilibration (Anderson and Olimpio, 1977; Lasaga *et al.*, 1977; Lasaga, 1983) and was the basis of the models in this paper. However, it has been argued that during prograde metamorphism, mineral growth and equilibration is controlled by either intergranular diffusion (Carlson, 1989) or by the kinetics of surface attachment (Loomis, 1982; Finlay and Kerr, 1987). These mechanisms could also be important or even rate-limiting steps for reactions that occur during cooling. Although my models have not considered these mechanisms, the rate laws for surface attachment and intergranular diffusion also involve thermally activated rate constants similar to the Fe–Mg interdiffusion constant (Lasaga, 1986). For this reason, the results of this modelling is probably also qualitatively applicable to re-equilibration by these mechanisms. If that is the case, then regardless of the mechanisation, as long as a single re-equilibration mechanism remains dominant, a closure temperature similar to the one described here should exist. Thus, major variations in the pressure and temperature recorded by thermobarometry could reflect changes in the re-equilibration mechanism as much as differences in tectonic or thermal history.

Acknowledgements

This work was carried out while P. Crowley was on leave at the Geologisches Institut, ETH-Zentrum and benefited from discussions with J. Connolly and N. Mancktelow. The visit to the ETH was funded in part by an Amherst College Trustee Fellowship.

References

Anderson, D. E. and Olimpio, J. C. (1977) Progressive homogenization of metamorphic garnets, south Morar, Scotland: evidence for volume diffusion. *Can. Mineral.*, **15**, 205–16.

Barker, A. J. and Anderson, M. W. (1989) The Caledonian structural metamorphic evolution of south Trom, Norway. In *Evolution of Metamorphic Belts* (Daly, J. S., Cliff, R. A., and Yardley, B. W. D., eds.), Geo. Soc. Lond. Spec. Publ., **43**, 385–9.

Buck, W. R., Martinez, F., Steckler, M. S., and Cochran, J. R. (1988) The thermal consequences of lithospheric extension: Pure and simple. *Tectonics*, **7**, 213–34.

Carlson, W. D. (1989) The significance of intergranular diffusion to the mechanics and kinetics of porphyroblast crystallization. *Contrib. Mineral. Petrol.*, **103**, 1–24.

Connolly, J. A. A. and Thompson, A. B. (1989) Fluid and enthalpy production during regional metamorphism. Ibid., **102**, 347–66.

Crank, J. (1975) *The Mathematics of Diffusion*. (2nd ed.), Clarendon Press, Oxford.

Crowley, P. D. (1988) The metamorphic break across postmetamorphic thrust faults: an unreliable indicator of structural throw. *Geology*, **16**, 46–9.

——(1990) Metamorphism with the Çokkul synform: evidence for detachment faulting within the metamorphic infrastructure of the Norwegian Caledonides (67°30′N). *J. metamorph. Geol.* in press.

——and Spear, F. S. (1987) The *P–T* Evolution of the Middle Köli Nappe Complex, Scandinavian Caledonides (68 N) and its Tectonic Implications, *Contrib. Mineral. Petrol.*, **95**, 512–22.

Cygan, R. T. and Lasaga, A. (1985) Self diffusion of magnesium in garnet at 750° to 900 °C. *Am. J. Sci.*, **285**, 328–50.

Davy, Ph. and Gillet, P. (1986) The stacking of thrust sheets in collisional zones and its thermal consequences. *Tectonics*, **5**, 913–30.

Dodson, M. (1973) Closure temperature in cooling geochronological and petrological systems. *Contrib. Mineral. Petrol.*, **40**, 259–74.

Elphick, S. C., Ganguly, J., and Loomis, T. P. (1985) Experimental determinations of cation diffusivity in aluminosilicate garnet I: Experimental methods and interdiffusion data. Ibid., **90**, 33–44.

England, P. C. and Richardson, S. W. (1977) The influence of erosion upon mineral facies of rocks from different metamorphic environments. *J. Geol. Soc. Lond.*, **134**, 210–3.

——and Thompson, A. B. (1984) Pressure–temperature–time paths of regional metamorphism I: Heat transfer during the evolution of regions of thickened crust. *J. Petrol.*, **25**, 894–928.

Essene, E. J. (1989) The current status of thermobarometry in metamorphic rocks. In *Evolution of Metamorphic Belts* (Daly, J. S., Cliff, R. A., and Yardley, B. W. D., eds.) Geol. Soc. Lond. Spec. Publ., **43**, 1–44.

Ferry, J. M. and Spear, F. S. (1978) Experimental calibration of the partitioning of Fe and Mg between garnet and biotite. *Contrib. Mineral. Petrol.*, **66**, 113–7.

Finley, C. A. and Kerr, A. (1987) Evidence for differences in the growth rates among garnets in peletic schists from northern Sutherland, Scotland. *Mineral. Mag.*, **51**, 569–76.

Fisher, G. W. (1978) Rate laws in metamorphism. *Geochim. Cosmochim. Acta*, **42**, 1035–50.

Freer, R. (1981) Diffusion in silicate minerals and glasses: a data digest and guide to the literature. *Contrib. Mineral. Petrol.*, **76**, 440–54.

Hodges, K. V. and Crowley, P. D. (1985) Error Estimation in Empirical Geothermometry and Geobarometry for Pelitic Systems. *Am. Mineral.*, **70**, 702–9.

——and McKenna, L. W. (1987) Realistic propagation of uncertainty in geologic thermobarometry. Ibid., **72**, 673–82.

——and Royden, L. (1984) Geologic thermobarometry of retrograded rocks: an indication of the uplift trajectory of a portion of the northern Scandinavian Caledonides. *J. Geophys. Res.*, **89**, 7077–90.

Koziol, A. M. and Newton, R. C. (1988) Recalibration of the anorthite breakdown reaction and improvement of the plagioclase–garnet–Al_2SiO_5–quartz geobarometer. *Am. Mineral.*, **73**, 316–23.

Lasaga, A. C. (1983) Geospeedometry: An extension of geothermometry. In *Kinetics and Equilibrium in Mineral Reactions* (Saxena, S. K., ed.), 81–114, Springer-Verlag, New York.

——(1986) Metamorphic reaction rate laws and the development of isograds. *Mineral. Mag.*, **50**, 359–73.

——Richardson, S. M. and Holland, H. D. (1977) The mathematics of cation diffusion and exchange between silicate minerals during retrograde metamorphism. In *Energetics of Geological Processes* (Saxena, S. K. and Bhattachanji, eds.) 353–88. Springer-Verlag, New York.

Loomis, T. P. (1982) Numerical simulations of the disequilibrium growth of garnet in chlorite-bearing aluminous pelitic rocks. *Can. Mineral.*, **20**, 411–23.

Mancktelow, N. (1985) The Simplon Line: a major displacement zone in the western Lepontine Alps. *Eclogae geol. Helv.*, **78**, 73–96.

Rice, A. H. N., Begins, R. E., Robunson, D., and Roberts, D. (1989) Thrust related metamorphic inversions in the Caledonides of north Norway. In *Evolution of Metamorphic Belts* (Daly, J. S., Cliff, R. A., and Yardley, B. W. D., eds.), Geol. Soc. London. spec. Publ., **43**, 413–21.

Ruppel, C., Royden, L., and Hodges, K. V. (1988) Thermal models of extensional tectonics: Applications to pressure–temperature–time histories of metamorphic rocks. *Tectonics*, **7**, 947–57.

Steltenpohl, M. G. and Bartley, J. M. (1987) Thermobarometric profile through the Caledonian nappe stack of Western Ofoten, North Norway. *Contrib. Mineral. Petrol.*, **96**, 93–103.

Thompson, A. B. and England, P. C. (1984) Pressure–temperature–time paths of regional metamorphism II: Their inference and interpretation using mineral assemblages in metamorphic rocks. *J. Petrol.*, **25**, 894–928.

Walther, J. V. and Wood, B. J. (1984) Rate and mechanism in prograde metamorphism. *Contrib. Mineral. Petrol.*, **88**, 246–59.

[*Manuscript received 16 February 1990: revised 8 June 1990*]